Mon. Not. R. Astron. Soc. **389,** 678–690 (2008) doi:10.1111/j.1365-2966.2008.13612.x

A general catalogue of extended objects in the Magellanic System

E. Bica,[1] C. Bonatto,[1⋆] C. M. Dutra[2] and J. F. C. Santos, Jr.[3]

[1]*Departamento de Astronomia, Universidade Federal do Rio Grande do Sul, Av. Bento Gonçalves 9500 Porto Alegre 91501-970 RS, Brazil*
[2]*Universidade Federal do Pampa – UNIPAMPA, Centro de Ciências da Saúde, Rua Domingos de Almeida, 3525, Bairro São Miguel, Uruguaiana 97500-009 RS, Brazil*
[3]*Departamento de Física, ICEx, Universidade Federal de Minas Gerais, Av. Antônio Carlos 6627 Belo Horizonte 30123-970 MG, Brazil*

Accepted 2008 June 18. Received 2008 June 18; in original form 2008 May 2

ABSTRACT

We update the Small Magellanic Cloud (SMC), Bridge and Large Magellanic Cloud (LMC) catalogues of extended objects that were constructed by members of our group from 1995 to 2000. In addition to the rich subsequent literature for the previous classes, we now also include H I shells and supershells. A total of 9305 objects were cross-identified, while our previous catalogues amounted to 7900 entries, an increase of ≈12 per cent. We present the results in subcatalogues containing 1445 emission nebulae, 3740 star clusters, 3326 associations and 794 H I shells and supershells. Angular and apparent size distributions of the extended objects are analysed. We conclude that the objects, in general, appear to respond to tidal effects arising from the LMC, SMC and Bridge. Number-density profiles extracted along directions parallel and perpendicular to the LMC bar, can be described by two exponential-discs. A single exponential-disc fits the equivalent SMC profiles. Interestingly, when angular-averaged number-densities of most of the extended objects are considered, the profiles of both Clouds do not follow an exponential-disc. Rather, they are best described by a tidally truncated, core/halo profile, despite the fact that the Clouds are clearly disturbed discs. On the other hand, the older star clusters taken isolately, distribute as an exponential disc. The present catalogue is an important tool for the unambiguous identification of previous objects in current CCD surveys and to establish new findings.

Key words: Magellanic Clouds.

1 INTRODUCTION

The Magellanic Clouds are fundamental galaxies for astrophysics owing, for example, to their proximity, chemical compositions, age distributions, star cluster structural properties and related dynamical evolution, and as two close-by interacting galaxies (e.g. Westerlund 1990; Da Costa 1991; Dieball, Müller & Grebel 2002; Piatti et al. 2002; Mackey & Gilmore 2003; Bekki & Chiba 2007). Schaefer (2008) reviews recent estimates of the distance to the Clouds and arrives at the values $d_{\rm LMC} \approx 50$ kpc and $d_{\rm SMC} \approx 60$ kpc.

More than 50 yr have elapsed since the first attempts to systematically catalogue extended objects in the Magellanic Clouds (e.g. the non-stellar emission nebulae of Henize 1956). We refer as extended objects the emission nebulae, star clusters, associations, and H I shells and supershells. Early catalogues of star clusters included brighter ones in the SMC (Kron 1956; Lindsay 1958) and LMC (Shapley & Lindsay 1963; Lyngå & Westerlund 1963). Fainter clusters with deeper photographic material were detected, for example, by Hodge & Sexton (1966) and Hodge (1986). Binary or multiple clusters are another characteristics of many Magellanic Cloud clusters, showing their importance for cluster dynamical evolution (Bhatia & Hatzidimitriou 1988; de Oliveira et al. 2000). Examples of catalogues of associations are Lucke & Hodge (1970) for the Large Magellanic Cloud (LMC), Hodge (1985) for the Small Magellanic Cloud (SMC) and Battinelli & Demers (1992) in the Bridge. A complementary study to Henize (1956) is the catalogue of nebular complexes by Davies, Elliott & Meaburn (1976) based on Hα plates.

Hubble Space Telescope (*HST*) instrumention revealed serendipitously two faint clusters in the LMC bar that were undetected in Sky Survey plates (Santiago et al. 1998). These two clusters suggested the existence of an important undetected faint population of clusters. CCD mosaics, for example, Pietrzynski et al. (1998) in the SMC central parts, started to unveil that elusive cluster population.

Bica & Schmitt (1995, updated in Bica & Dutra 2000) and Bica et al. (1999) compiled general catalogues from numerous previous catalogues and many lists sparsely distributed in the literature, and presented new findings based on Sky Survey plates. The total number of extended objects in these catalogues is 7900, including the SMC, intercloud (Bridge) region, and LMC. Cross-identifications

⋆E-mail: charles@if.ufrgs.br

Table 1. New clusters and associations.

Reference (1)	Analysed number (2)	New objects (3)	Acronym (4)
Testor, Llebaria & Debray (1988)	1	1	TLB
Walborn & Blades (1997)	5	1	WB
Walborn et al. (1999a)	2	2	WBB
Walborn et al. (1999b)	4	1	WDP
Walborn, Maí z-Apellániz & Barbá (2002)	5	3	WMB
Heydari-Malayeri et al. (1999)	3	1	HCD99-
Heydari-Malayeri et al. (2000)	2	1	HRR
Heydari-Malayeri et al. (2001)	1	1	HCD01-
Heydari-Malayeri et al. (2001)	2	1	HCD02-
Heydari-Malayeri, Meynadier & Walborn (2003)	2	2	HMW
Meynadier, Heydari-Malayeri & Walborn (2005)	1	1	MHW
Bellazzini, Pancino & Ferraro (2005)	1	1	Bologna
Nota et al. (2006); Sabbi et al. (2007)	16	16	NSS
Nakajima et al. (2005)	25	18	NKD
Testor et al. (2006)	2	2	TLF
Testor et al. (2007)	2	2	TLK
Pietrzynski et al. (1999)	615	126	LOGLE
Gouliermis et al. (2003) – Clusters	259	125	GKK-O
Gouliermis et al. (2003) – Associations	153	102	GKK-A
Gouliermis, Quanz & Henning (2007)	5	5	GKH
Hennekemper et al. (2008)	5	0	HGH
Schmalzl et al. (2008)	1	1	SGDH

Note. Otherwise stated, objects are essentially all clusters.

that take into account object plate identifications, class, size, positions and uncertainties were carried out.

As present-day Magellanic Cloud Surveys provide their first results, like the University of Michigan UM/CTIO Magellanic Cloud Emission Line Survey (MCELS),[1] or are scheduled for soon, such as the Visible and Infrared Survey Telescope for Astronomy (VISTA),[2] we found it timely to update the catalogues of Bica et al. (1999) and Bica & Dutra (2000), so that literature objects can be easily identified, and new findings in deeper surveys can be confidently asserted.

Besides the update, we will use the present catalogue to investigate structural properties of the Clouds as probed by the large-scale spatial distribution of different classes of objects. We will also examine potential effects of the LMC, SMC and Bridge tidal fields on the structure of individual objects.

This paper is structured as follows. In Section 2, we present the updates and additions to the Magellanic System catalogue. In Section 3, we discuss statistical properties of the different object classes contained in the catalogue, such as the distributions of apparent size and ellipticity. In Section 4, we examine dependences of the object parameters with distance to the Clouds centroids. In Section 5, we investigate the structure of both Clouds with the spatial distribution of the catalogue objects. Concluding remarks are given in Section 6.

2 THE UPDATED CATALOGUE

The procedures used in this paper are essentially the same as those employed in our previous ones. We cross-identify new and old objects by position, angular size, and object class. We give in Table 1 the statistics on clusters and associations (and related objects) from papers published since the latest catalogue version. Most new papers deal with discoveries with HST. A large number of LMC clusters were studied in the central parts by Pietrzynski et al. (1999) as part of the Optical Gravitational Lens Experiment (OGLE; Udalski 2003). We also included information from Pietrzynski & Udalski (1999) dealing with SMC clusters, and about binary and multiplet clusters in the LMC from Pietrzynski & Udalski (2000).

Besides those, the updated catalogue includes 10 new findings (four clusters, three associations, and three emission nebulae) under the acronym BBDS.

A new feature of the present catalogue is the literature indications of genuine (age $>$ 9 Gyr) globular clusters (GCs), with two in the SMC (Olszewski, Aaronson & Schommer 1987; Mighell, Sarajedini & French 1998; Alcaino, Alvarado & Kurtev 2003) and 16 in the LMC (Dutra et al. 1999; Mackey & Gilmore 2004; Mackey, Payne & Gilmore 2006). From the latter study we include ESO 121-SC3 as an LMC GC, which is the only cluster in the 4–9 Gyr LMC age gap. They suggest that ESO 121-SC3 was accreted by the LMC. Also included are old SMC intermediate age clusters (IACs) at 4–9 Gyr. These studies are Da Costa (1999), Crowl et al. (2001), Piatti et al. (2001, 2005) and Piatti et al. (2007). Known GCs and old IACs are very useful to trace the old systems of the Magellanic Clouds (Section 3).

The previous catalogue versions included 46 SNRs. Now there are 74 SNRs and candidates. The sources were Dickel et al. (2001), Lazendic, Dickel & Jones (2003), van der Heyden, Bleeker & Kaastra (2004), Blair et al. (2006), Williams, Chu & Gruendl (2006), Bojicic et al. (2007), and Chu et al. (1997).

The catalogue includes improved coordinates derived with DSS and XDSS[3] images for star clusters in the Bridge and in the outer

[1] http://www.ctio.noao.edu/mcels/

[2] http://www.eso.org/gen-fac/pubs/messenger/archive/no.127-mar07/arnaboldi.pdf

[3] Extracted from the Canadian Astronomy Data Centre (CADC), at http://cadcwww.dao.nrc.ca/

Table 2. SMC, Bridge and LMC extended object census.

Object type (1)	Census (2)	Comments (3)
Star clusters	3740	C+CN+CA+DCN
C	2769	Ordinary cluster
CN	91	Cluster in nebula
CA	861	Cluster similar to association
DCN	18	Decoupled cluster from nebula
Associations	3326	A+AN+AC+DAN
A	1724	Ordinary association
AN	257	Association w/nebular traces
AC	1253	Association similar to cluster
DAN	92	Decoupled association from nebula
Emission Nebulae	1445	NA+NC+EN+SNR+DNC+DNA
NA	995	Nebula w/embedded association
NC	260	Nebula w/probable embedded cluster
EN	6	Nebula wo/association/cluster
SNR	74	Supernova remnants
DNC	18	Decoupled nebula from cluster
DNA	92	Decoupled cluster from nebula
H I shells(HS)	794	H I shells and supershells

parts of the SMC. Several corrections were made throughout the previous catalogues, such as for example, for LMC-N34A and LMC-N34B.

As another interesting case, Lindsay (1961) discovered the nebula L61-593 associated to an emission-line star in the SMC Wing. Westerlund & Henize (1963) interpreted it as a B star with mass loss. With the DSS B and XDSS R images, we find that a star cluster appears to be present, now favouring L61-593 as an H II region rather than a mass-loss star.

In Table 2, we show the updated census of the extended objects in the Magellanic System.

In electronic form, Tables 3–6 contain, respectively, 3740 star clusters, 3326 associations, 1445 emission nebulae and 794 H I shells and supershells. The SMC shells and supershells were studied by Hatzidimitriou et al. (2005) and Staveley-Smith et al. (1997). Hatzidimitriou et al. (2005) pointed out 59 empty shells that do not appear to have stellar counterpart. Such objects are also indicated in Table 5. Muller et al. (2003) presented shells and supershells in the western part of the Bridge, while Kim et al. (1999) presented those detected in the LMC. The electronic tables are arranged as follows, by column: (1) designations; (2) and (3) the central coordinates $\alpha(J2000)$ and $\delta(J2000)$, respectively; (4) object class (see definitions in Table 2); (5) and (6) major and minor diameters (a and b, in arcmin), respectively; (7) position angle (PA, in degrees), with $PA = 0^\circ$ to the north and $PA = +90^\circ$ to the east and (8) object classification, where 'mP', 'mT', 'm4', and so on, mean member of a pair, triplet, and so forth. For details see, e.g. Bica et al. (1999). Excerpts of the electronic tables showing the first five entries are given in Tables 3–6.

We have checked with the present catalogue spatial coincidences between clusters or associations with the above empty shells. Except for a couple of new coincidences, the vast majority of these shells remain empty. Interestingly, a significant fraction of the empty shells distribute over a protuberance to the NE of the SMC, possibly an incipient tidal tail. This protuberance shows up in the Hatzidimitriou et al. (2005) study. A possible interpretation is that these empty shells are not related to recently formed stars. Instead, they might be the first stages of the gravitational collapse leading to a molecular cloud and/or to star cluster formation.

Also included are H II regions in the Bridge that Muller & Parker (2007) cross-identified with associations from Bica & Schmitt (1995), Bica & Dutra (2000) and probable UV ionising stellar sources (FAUST – Bowyer et al. 1995).

In this study, we adopt shorter acronyms for frequent objects for the sake of space, inspired on SIMBAD[4] designation contractions: SMC-DEM becomes DEMS, LMC_DEM is now DEML, SMC_OGLE is SOGLE and LMC_OGLE is LOGLE. In general, we adopt the authors initials as acronym, likewise SIMBAD. SIMBAD designations include the year of publication, and have the advantage to be unique, but often they are too long for a study like the present one. We also changed the BD designation of associations in the Bridge in our previous papers to ICA (intercloud association) according to Battinelli & Demers (1992) and Muller & Parker (2007).

The identification of DEML 147 as an emission nebula on the LMC bar is supported by the detection of a UV-bright cluster or association by Gouliermis et al. (2003), and is thus included in the present catalogue.

With the recent additions and cross-identifications, the present catalogue contains about 12 per cent more objects than those in Bica et al. (1999) and Bica & Dutra (2000) together.

Fig. 1 shows the angular distribution of the total sample of extended objects. Outstanding features such as the LMC central disc and bar ($PA \approx 100^\circ$), outer decentred ring, the Bridge and the SMC Wing and disc ($PA \approx 50^\circ$), have been discussed in, for example, Westerlund (1990), Kontizas et al. (1990), Bica & Schmitt (1995), Bica et al. (1999) and Bica & Dutra (2000), and references therein.

In Fig. 1 the old LMC clusters trace a bar-like structure, somewhat rotated with respect to that defined by the extended objects in general. This effect was previously described by Dottori et al. (1996), where they found that the bar occupied preferentially by young clusters (SWB I) is rotated with respect to the older group (SWB II), owing to the propagation of the perturbation through the LMC disc that causes current star formation.

In Fig. 2, we show separate distributions for each individual class. We note that the LMC is still undersampled with respect to the SMC H I shells and supershells, and the eastern part of the Bridge is yet to be observed. Besides the SMC bar and Wing, the H I shells may trace additional features possibly related to tidal effects. Interestingly, the associations suggest a spiral arm-like outer extension in the eastern side of the LMC. The SMC disc and the Bridge are better traced by associations. The nebulae in the LMC appear to follow a spiral pattern centred in the 30 Dor region (Fig. 2, lower left-hand panel). Finally, the old star clusters trace the LMC bar and outer parts, while the old SMC clusters are preferentially distributed in its outer parts.

3 STATISTICAL PROPERTIES OF THE EXTENDED OBJECTS

The relatively large number of objects included in the subsamples (electronic Tables 3–6), can be used to investigate statistical properties of some structural parameters, both in terms of object class and tidal field strength. Of particular interest is whether effects due to the very different LMC and SMC tidal fields on the structural parameters and spatial distribution of the objects can be detected and quantified with the presently updated catalogue.

[4] http://simbad.u-strasbg.fr/simbad/

Table 3. Sample of table of star clusters.

Object	$\alpha(J2000)$ (h m s)	$\delta(J2000)$ (° ′ ″)	Type	a (arcmin)	b (arcmin)	PA (°)	Comments
(1)	(2)	(3)	(4)	(5)	(6)	(7)	(8)
AM-3, ESO 28SC4	23:48:59	−72:56:43	C	0.90	0.90	–	Old IAC
L1, ESO 28SC8	0:03:54	−73:28:19	C	4.60	4.60	–	Globular Cluster
L2	0:12:55	−73:29:15	C	1.20	1.20	–	
L3, ESO 28SC13	0:18:25	−74:19:07	C	1.00	1.00	–	
HW1	0:18:27	−73:23:42	CA	0.95	0.85	0	

Notes. See Supporting Information section for details of the full table. Col. 4: object type as defined in Table 2. Cols. 5 and 6: major and minor axes. Col. 7: major axis position angle.

Table 4. Sample of table of associations.

Object	$\alpha(J2000)$ (h m s)	$\delta(J2000)$ (° ′ ″)	Type	a (arcmin)	b (arcmin)	PA (°)	Comments
(1)	(2)	(3)	(4)	(5)	(6)	(7)	(8)
B3	0:24:00	−73:38:10	A	1.20	1.10	40	
HW2	0:27:57	−74:00:05	C	0.75	0.55	70	
H86-3	0:28:04	−73:03:33	AC	0.75	0.55	70	
H86-6	0:29:22	−73:00:00	AC	0.60	0.45	20	
HW3	0:29:54	−73:42:03	AC	1.50	1.10	70	

Notes. See Supporting Information section for details of the full table. Col. 4: object type as defined in Table 2. Cols. 5 and 6: major and minor axes. Col. 7: major axis position angle.

Table 5. Sample of table of emission nebulae.

Object	$\alpha(J2000)$ (h m s)	$\delta(J2000)$ (° ′ ″)	Type	a (arcmin)	b (arcmin)	PA (°)	Comments
(1)	(2)	(3)	(4)	(5)	(6)	(7)	(8)
SMC-N3,DEMS1	0:31:40	−73:47:43	NA	1.10	1.10	–	
DEMS2	0:37:15	−72:59:41	DNA	1.80	1.20	140	in H-A1, DC K14
DEMS5	0:41:00	−73:36:22	NA	2.90	2.90	–	
DEMS6	0:42:14	−72:59:25	NA	1.10	1.10	–	
L61-34,MA37	0:42:16	−72:59:53	NC	0.40	0.35	120	in DEMS6

Notes. See Supporting Information section for details of the full table. Col. 4: object type as defined in Table 2. Cols. 5 and 6: major and minor axes. Col. 7: major axis position angle.

Table 6. Sample of table of H I shells and supershells.

Object	$\alpha(J2000)$ (h m s)	$\delta(J2000)$ (° ′ ″)	Type	a (arcmin)	b (arcmin)	PA (°)	Comments
(1)	(2)	(3)	(4)	(5)	(6)	(7)	(8)
SSH-GS1	0:31:26	−72:52:24	HS	5.4	5.4	–	
SSH-GS2	0:32:07	−73:21:19	HS	5.8	5.8	–	
SSH-GS3	0:32:15	−72:49:46	HS	2.6	2.6	–	
SSH-GS4	0:33:07	−73:26:16	HS	11.6	11.6	–	
SSH-GS5	0:33:09	−73:23:17	HS	4.8	4.8	–	

Notes. See Supporting Information section for details of the full table. Col. 4: object type as defined in Table 2. Cols. 5 and 6: major and minor axes. Col. 7: major axis position angle.

For the sake of simplicity, we separate the objects into two classes, (i) clusters, which contain essentially the star clusters older than 5 Myr and (ii) associations and related objects, in which we gather the H I shells and supershells, OB associations and emission nebulae. Besides, we also consider the spatial location of each object according to right ascension. We take as SMC objects those located within $23^{\rm h}40^{\rm m} < \alpha(J2000) < 01^{\rm h}20^{\rm m}$, LMC ones at $4^{\rm h} < \alpha(J2000) < 6^{\rm h}40^{\rm m}$, while Bridge objects are located in between (e.g. Fig. 1). We point out that the present definition of the Bridge is somewhat broader than that adopted in Bica & Schmitt (1995). It now includes part of the SMC Wing.

3.1 Apparent diameters

The updated MC catalogue gives the apparent major and minor axes, a and b, respectively, from which we compute the mean apparent diameter $D_{\rm app} = (a + b)/2$ for each object. Based on this, we build the apparent diameter distribution function, defined as

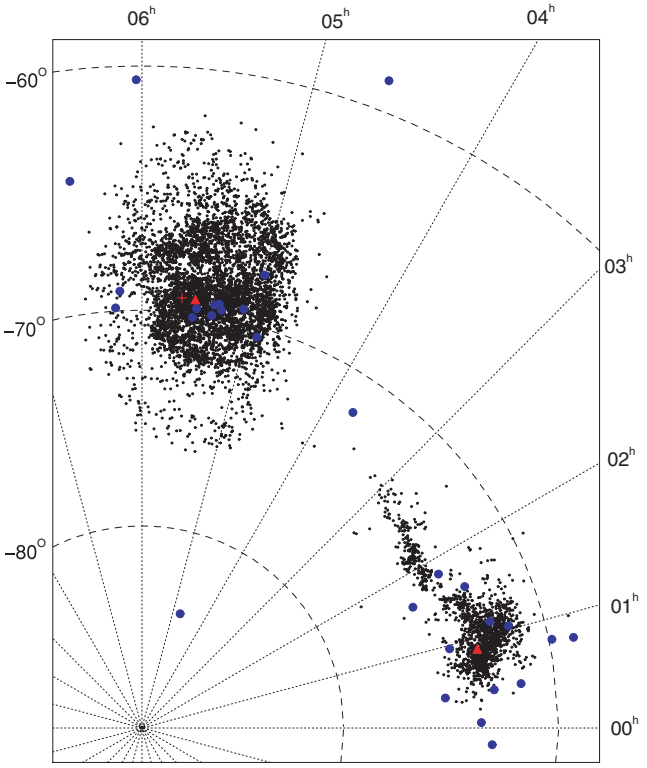

Figure 1. Angular distribution of the 9305 extended objects in the Magellanic System. Clusters older than 4 Gyr are shown as large blue circles. The derived LMC and SMC centroids (see Table 8) are indicated by red triangles. The position of 30 Dor is shown by the plus sign.

$\phi(D_{\rm app}) = {\rm d}N/{\rm d}D_{\rm app}$. In Fig. 3 (left-hand panels), we show $\phi(D_{\rm app})$ of the clusters and associations located in the LMC, SMC and Bridge, as well as in the MC system as a whole. Star clusters and associations present different distributions in all MC subsystems. In particular, associations tend to have objects with larger diameters than the clusters.

Another interesting fact is that the apparent diameter distributions fall off as a power law for objects that occupy the large-size tail (Fig. 3). Indeed, the distributions can be reasonably well fitted with the function $\phi(D_{\rm app}) \sim D_{\rm app}^{-\eta}$ in the range $D_{\rm app}^{\rm min} \leq D_{\rm app} \leq D_{\rm app}^{\rm max}$ (Fig. 3). Table 7 summarizes the fit details. The number of LMC and SMC star clusters fall off towards large diameters at a faster rate ($\sim D_{\rm app}^{-3.4}$) than the associations ($\sim D_{\rm app}^{-2}$), while in the Bridge the slopes are similar ($\sim D_{\rm app}^{-2}$). The slope in the apparent radii distribution of the associations agrees with that predicted (and measured) for H II regions in spiral galaxies (Oey et al. 2003). Since most of the clusters are significantly older than the associations, the difference in slope (and maximum size) probably reflects the several million years of dynamical evolution and disruption effects operating on the former structures. Besides, the steeper decline with apparent diameter observed in the LMC and SMC cluster $\phi(D_{\rm app})$, with respect to the Bridge, is consistent with the stronger tidal field of the Clouds.

If extrapolated to the small-radii tail, the decaying-power law distribution of apparent diameters in the LMC, SMC and Bridge (top left-hand panel in Fig. 3), would suggest that the number of observed objects represents a small fraction of the total population. Indeed, because of the difference in slope, the fraction of observed associations would be ∼2.7, and ∼0.6 per cent for the clusters. Known small clusters are in general embedded in H II region complexes (Table 1). Their small number certainly stresses the fact that systematic surveys for small-scale structures are yet to be carried out.

The apparent diameter distribution functions (normalized to the same number of objects for interclass comparisons) of similar classes of objects in the LMC, SMC and Bridge, are shown in Fig. 4 (top panels). For a more intrinsic analysis, SMC and Bridge apparent diameters have been multiplied by 1.2, to account for the different distances with respect to the LMC (Section 1). Within uncertainties, the star clusters present similar distributions, especially in the LMC and SMC. With the available data, the Bridge appears not to harbour clusters smaller than $D_{\rm app} \lesssim 0.3$ arcmin. As for the H I shells, associations and nebulae, the SMC and Bridge present similar distributions, and both appear to have an excess of objects larger than $D_{\rm app} \approx 2$ arcmin with respect to the LMC. This effect may be associated to the weaker SMC and Bridge tidal fields, which allow the presence of distended, low-binding energy objects, such as those included in the association class. The LMC and SMC distributions present a steep drop towards smaller $D_{\rm app}$, beginning at $D_{\rm app} \approx 0.5$ arcmin. At the LMC and SMC distances, this corresponds to physical radii of ≈4 pc. Such clusters (or associations) are not small by Galactic open cluster standards. In fact, this corresponds to average-size Galactic open clusters (see, e.g. fig. 7 in Bonatto et al. 2007). This raises the question of whether such a drop is a real effect associated to formation processes and/or dissolution, an observational limitation linked to completeness, or more probably, a combination of both. In any case, the completeness is not the same in the 3 MC subsystems. Because of the lower surface brightness of the background and the less-populous nature of the Bridge, star clusters and associations stand out more, and completeness effects in the Bridge are expected to be less important than in the Clouds.

At this point, it may be interesting to compare the MCs apparent diameter distribution functions with the equivalent one built with the Galactic population of GCs, which is basically complete and probes all the old Galactic substructures (see, e.g. Bonatto et al. 2007). Obviously, the Galactic GCs are essentially old systems, while the MCs distribution functions contain young objects as well. However, the main purpose here is to examine the shape of the Milky Way (MW) GC size-distribution function, especially at the small-size tail. In principle, it should be more correct to include the Galactic open clusters in this analysis, since they span a wide range in ages and populate especially the young tail of the age distribution. However, contrary to the GCs, the open clusters are severely affected by completeness, especially at the faint-end of the luminosity distribution (e.g. Bonatto et al. 2006a), which might introduce a completeness-related drop towards small open clusters in the size distribution function.

Thus, with the above arguments in mind, we take as reference of GC size the tidal radii given by (Harris 1996, and the update in 2003[5]). Additionally, we consider as well the tidal radii of 11 faint GCs (not included in Harris 1996) derived by Bonatto & Bica (2008), and the recently studied GC FSR 1767 (Bonatto et al. 2007). Since MCs objects are essentially at the same distance from the Sun, the MW GC tidal radii are converted to the parsec scale for a consistent comparison. The latter conversion is based on the updated GC distances to the Sun given by Bica et al. (2006). For comparison purposes, the dynamical range of the MW GCs tidal radii have matched to the angular scales of the MCs (Fig. 4).

[5] http://physun.physics.mcmaster.ca/Globular.html

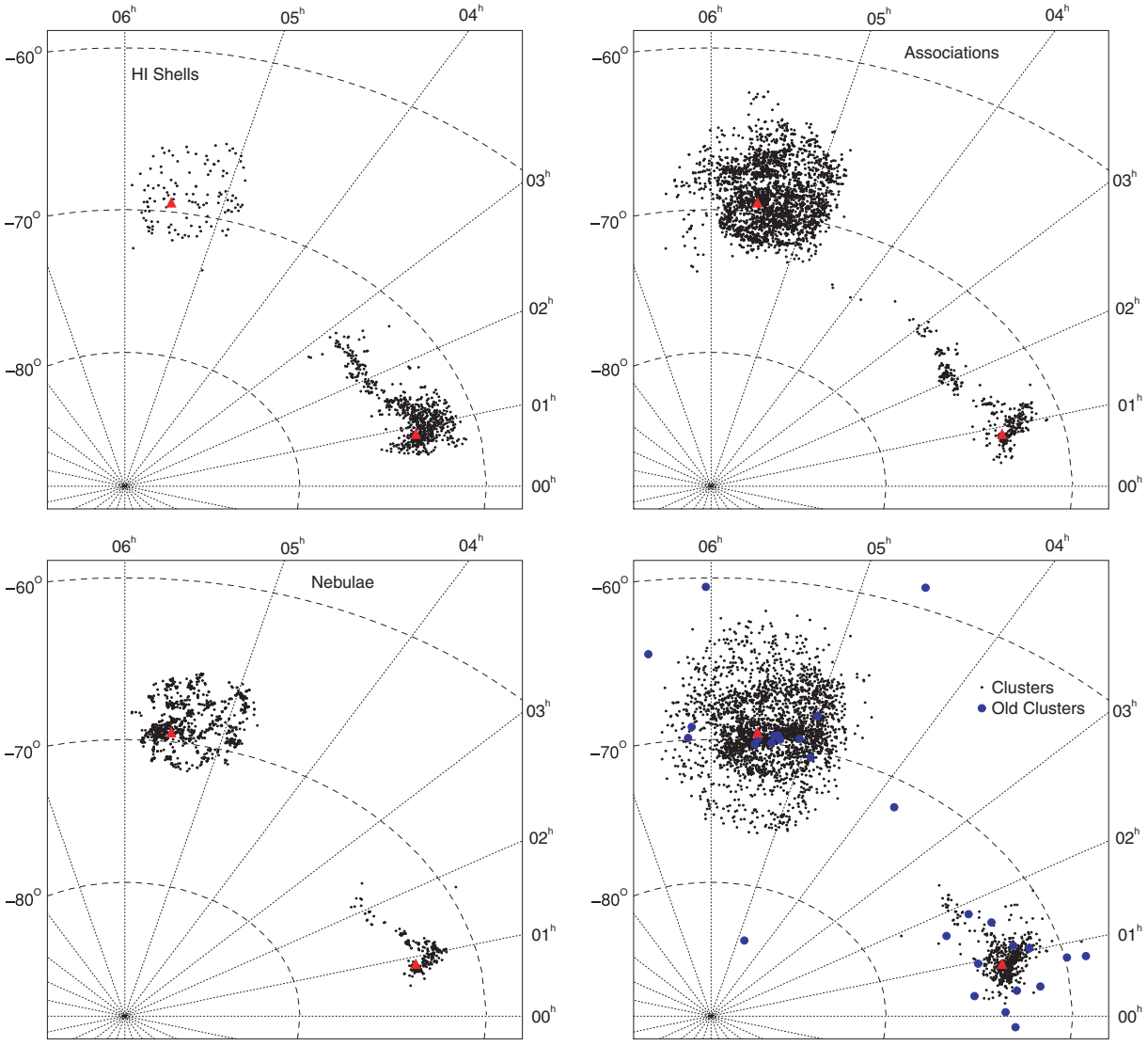

Figure 2. Angular distribution of the H I shells and supershells (top left-hand panel), stellar associations (top right-hand panel), emission nebulae (bottom left-hand panel), and star clusters (bottom right-hand panel). The adopted LMC and SMC centroids are indicated in all panels by filled triangles.

The tidal radii distribution function of the MW GCs is shown in Fig. 4 (bottom panel). Qualitatively, it presents similar features as those of the MCs objects, especially the relatively narrow width of the MC star clusters distribution function. Besides a maximum between $16 \lesssim R_{\rm t}({\rm pc}) \lesssim 30$, the distribution function of the Galactic GCs drops off both towards small and large radii. If the MW GCs sample is indeed basically complete, this suggests that the small-size drop observed in the MCs distribution functions may be real, at least in part.

The peak distribution of apparent diameters in the MC system occurs for $D_{\rm app} = 0.53$–0.77 arcmin which, for an average distance of ≈55 kpc, corresponds to radii in the range ≈4.2–6.2 pc. Such radii are a factor ∼4–5 smaller than the peak tidal radii of the MW GCs. Most of the difference may be accounted for by the fact that we deal with apparent sizes (measured on images as far as the background limit) in the MC system and tidal radii (which comes from, e.g. a King-profile fit) in the MW. Although most of the cluster stars can be considered to be contained inside the apparent radius, it is smaller than the tidal radius. For instance, the tidal radii computed for populous and relatively high Galactic latitude MW OCs such as M 67, NGC 188 and NGC 2477, are about four times larger than the respective apparent radii (Bonatto & Bica 2005).

3.2 Ellipticity

We apply a similar analysis to the ellipticity ($e = 1 - b/a$) distribution function, $\phi(e) = {\rm d}N/{\rm d}e$. LMC, SMC and Bridge clusters follow similar distribution functions (Fig. 3, right-hand panels), especially the LMC and SMC ones. The fractional number of clusters decreases monotonically with ellipticity within the range $0.03 \lesssim e \lesssim 0.45$, in all structures considered.

While the ellipticity distribution function of the clusters is similar in the LMC, SMC and Bridge, the associations, on the other hand, have different properties in different spatial structures. In particular, LMC and SMC associations contain objects with higher ellipticity values ($0.03 \lesssim e \lesssim 0.8$) than those of the clusters, with a slower decay of the fractional number with increasing e (Fig. 3).

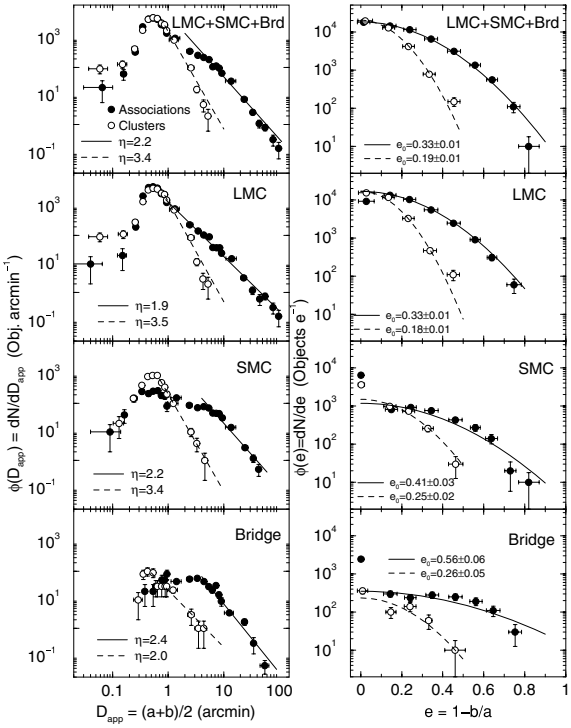

Figure 3. Left-hand panels: apparent diameter distribution function, $\phi(D_{\rm app}) = {\rm d}N/{\rm d}D_{\rm app}$, of the star clusters and associations. LMC, SMC and Bridge distributions are shown separately, as well as these three spatial structures together (top most panel). Fits of $\phi(D_{\rm app}) \sim D_{\rm app}^{-\eta}$ to the large-size tail are shown for the associations (solid line) and clusters (dashed). Right-hand panels: same as the left ones for the ellipticity ($e = 1 - b/a$) distribution function, $\phi(e) = {\rm d}N/{\rm d}e$. Fits in the right-hand panels correspond to the exponential-decay function $\phi(e) \sim e^{-(e/e_0)^2}$.

Table 7. Properties of the large-size tail of $\phi(D_{\rm app})$.

Reference sample	$D_{\rm app}^{\rm min}$ (arcmin)	$D_{\rm app}^{\rm max}$ (arcmin)	ϕ_0	η
All assoc.	4.4	100	7119 ± 1583	2.2 ± 0.1
All clusters	0.76	5.3	1774 ± 160	3.4 ± 0.2
LMC assoc.	0.95	100	1439 ± 87	1.9 ± 0.1
LMC clusters	0.76	5.3	1516 ± 162	3.5 ± 0.2
SMC assoc.	5.4	43	3181 ± 1098	2.2 ± 0.1
SMC clusters	0.76	4.6	209 ± 7	3.4 ± 0.1
Bridge assoc.	4.4	55	1789 ± 687	2.4 ± 0.2
Bridge clusters	0.54	4.4	22 ± 3	2.0 ± 0.2

Notes. Fits with the function $\phi(D_{\rm app}) = \phi_0\, D_{\rm app}^{-\eta}$ are performed for $D_{\rm app}^{\rm min} \leq D_{\rm app} \leq D_{\rm app}^{\rm max}$. The combined LMC, SMC and Bridge samples are represented by the 'All' reference sample.

Bridge associations have an ellipticity distribution that is rather flat in the range $e \sim 0.1 - 0.5$, which indicates the presence of an important fraction of non-circular objects. Besides, the distribution reaches a peak for the nearly circular objects. SMC associations follow a similar, although less flat, distribution. LMC associations, on the other hand, follow a smoothly decreasing distribution, with a peak at $e \approx 0.15$, and dropping somewhat at $e = 0$. Besides, LMC, SMC and Bridge associations reach significantly higher values of e than the corresponding clusters, $e \lesssim 0.8$.

Analytically, the combined LMC+SMC+Bridge ellipticity distribution functions for the associations and clusters (Fig. 3, top

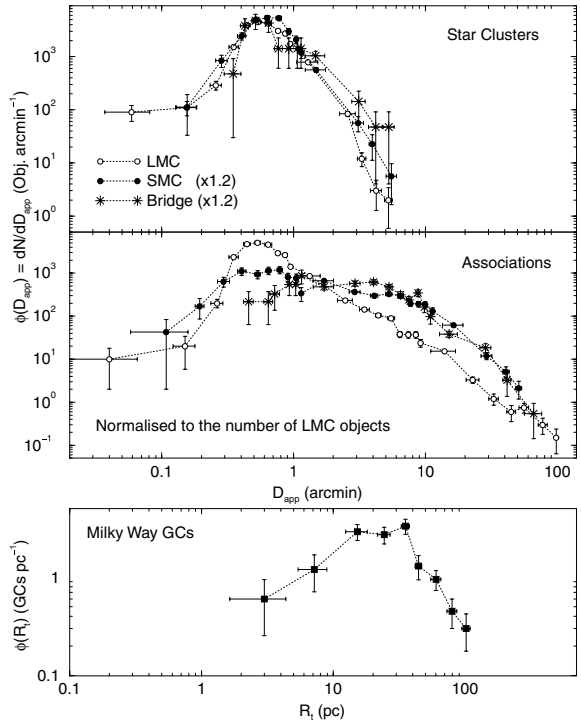

Figure 4. Top panels: apparent diameter distribution function of the LMC, SMC and Bridge built with star clusters (top panel) and associations (middle panel). SMC and Bridge apparent diameters have been multiplied by 1.2 to correct for the different distances with respect to the LMC. These functions have been normalized to the LMC number of objects. Bottom panel: tidal radius distribution function of the Milky Way GCs, in absolute scale. For a consistent comparison with the MCs apparent diameters, the dynamical range of the abscissa is equal in all panels.

right-hand panel) are well described by the function $\phi(e) \sim e^{-(e/e_0)^2}$, with dimensionless ellipticity scales $e_0 = 0.33 \pm 0.01, 0.19 \pm 0.01$, respectively. Given the relative similarity of the remaining, isolated distribution functions in the LMC, SMC and Bridge with the combined ones, it is obvious that they follow the same analytical function, but with different ellipticity scales. Indeed, the best-fitting functions (Fig. 3, right-hand panels) are obtained for association-ellipticity scales about twice larger than those of the clusters. While the cluster ellipticity scale increases ≈44 per cent from the LMC to the SMC and Bridge, e_0 for the associations increases by ≈70 per cent.

The above aspects are consistent with the fact that associations, in general, tend to be systems less-bound than clusters, and thus more subject to distortions by tidal fields. Besides, strong tidal fields may prevent the survival to advanced ages of a large population of distended objects, because of induced torques, tidal disruption, and so on. With time, such effects may either disrupt significantly distended objects, or at least, make them more circular at later ages. In any case, the qualitative aspects of the ellipticity distribution functions, as well as the environmental dependence of the ellipticity-scale, appear to correlate with the relative strengths of the LMC, SMC and Bridge tidal fields.

3.3 Position angle and alignment

In Fig. 5, we examine the distribution of the position angle (*PA*) of the clusters and associations around both Clouds. Objects with

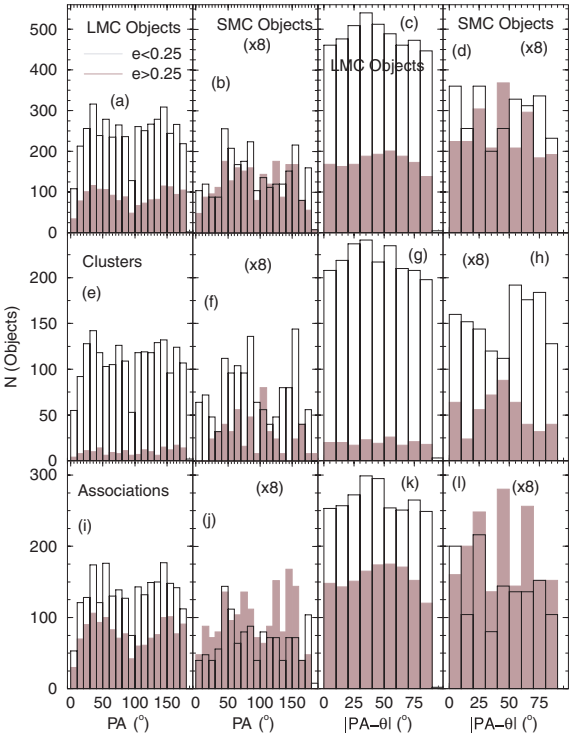

Figure 5. Histograms of the position angle and alignment angle measured in the LMC and SMC objects. Ellipticities larger (shaded histograms) and smaller (white) than $e = 0.25$ are considered separately. Note that the SMC histograms have been multiplied by 8 for visualization purposes.

ellipticity higher and lower than $e = 0.25$ are considered separately. In the LMC, ≈92 per cent of the clusters with *PA* measured are more circular than $e = 0.25$ (panel e), while in the SMC this fraction drops to ≈74 per cent (f). As for the associations, the corresponding fractions are ≈63 per cent in the LMC (i) and ≈42 per cent in the SMC (j). Clusters, in both Clouds, tend to be more circular than the associations, especially in the LMC, which again is consistent with the respective tidal field strengths of the Clouds, and the relative binding energy of the objects. Interestingly, there is a significant drop in the number of LMC objects with $PA \approx 100^\circ$, especially the associations, but conspicuous as well for the $e \lesssim 0.25$ clusters. Since the *PA* of the LMC bar (Fig. 1) is on average ≈100° (Fig. 1), one might speculate whether there is an enhanced dissolution of objects with *PA* parallel to the bar. We expect that the maximum tidal effect will occur for extended objects at the tips of the bar with parallel *PA*, which might imply a resonant effect. The collapse of molecular clouds is expected to be essentially radial, so that clusters do not acquire much rotation during formation. Indeed, the bar/*PA* alignment does not occur in the SMC, probably because of its less prominent bar.

We also estimate the alignment between each object's *PA* and the angle defined by direction vector (θ) with respect to the corresponding Cloud centroid, $|PA - \theta|$. The angle θ is measured in the same way as *PA* (Section 2). Since the alignment is symmetrical with respect to the sign of $PA - \theta$, and corresponds to the smaller angle, the measured values are in the range $0^\circ \leq |PA - \theta| \leq 90^\circ$. Clusters and associations of both Clouds (Fig. 5, panels c, d, g, h, k and l) do not appear to present statistically significant trends in $|PA - \theta|$.

4 PARAMETERS AS A FUNCTION OF DISTANCE TO THE CENTROIDS

Most MW GCs have a size that scales with the Galactocentric distance (e.g. van den Bergh, Morbey & Pazder 1991; Bonatto & Bica 2008). Part of this relation may have been established as early as at the Galaxy formation, when the higher density of molecular gas in central regions may have produced smaller clusters (e.g. van den Bergh et al. 1991). Dynamical evolution, especially that driven by external processes such as tidal disruption, collision with giant molecular clouds, disc and spiral arms, is important as well to establish a relation of increasing cluster size with Galactocentric distance. Such processes lead to the disruption of most star clusters in a mass-dependent time-scale shorter than ≈1 Gyr (Gieles et al. 2006). Since the latter effects are more critical for low-mass objects located close to strong tidal fields, a similar relation has been observed for the Galactic open clusters (e.g. Lyngå 1982; Tadross et al. 2002; Bonatto & Bica 2005, 2007).

In the top panels of Fig. 6, we investigate the above issue with the apparent diameters of the catalogue LMC and SMC objects (converted to the values corresponding to the LMC distance). The main purpose here is to search for trends, thus to minimize scatter we work with running averages, which correspond to the average value of a given parameter within bins usually containing 20 per cent of the number of objects in each sample. The result of this procedure are the fiducial lines shown in Fig. 6. While LMC and SMC clusters have, on average, similar sizes, SMC associations are larger, as already implied by Fig. 4. Clusters and associations in both Clouds appear to follow a trend of increasing apparent size with angular distance to the respective centroid, except perhaps for some fluctuation in the LMC associations.

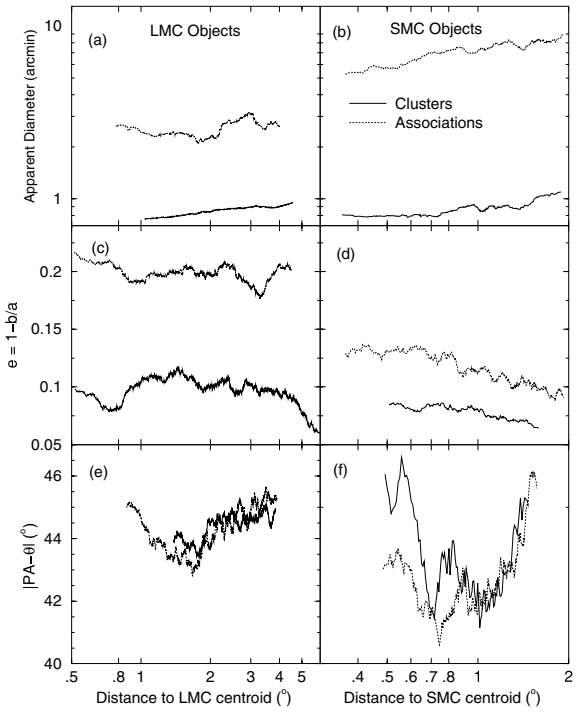

Figure 6. The average apparent diameter (top panels), ellipticity (middle panels) and alignment angle (bottom panels) of the LMC (left-hand panels) and SMC (right-hand panels) objects are examined as a function of the distance to the respective Cloud centroid. Curves correspond to fiducial lines. SMC apparent diameters have been converted to the values corresponding to the LMC distance.

The ellipticity of the SMC objects presents a similar relation with distance to the centroids, in the sense that objects closer to each Cloud's centroid tend to be less circular (middle right-hand panels of Fig. 6). However, this relation is milder in the LMC objects.

Finally, there appears to exist a mild correlation between the alignment angle and distance from the centroid for the LMC star clusters, in the sense that clusters closer to the LMC have the *PA* more aligned with the direction axis (bottom panels of Fig. 6). The alignment, in this case, occurs at the angle $|PA - \theta| \approx 45^\circ$. A similar relation appears for the LMC associations and SMC associations and clusters, but only for objects more distant than $\approx 1.5^\circ$ (LMC) and $\approx 0.7^\circ$ (SMC). The trend appears to be reversed for objects closer than these distances. However, as a caveat we note that such trends are rather speculative, since variations of $\approx 3^\circ$ and $\approx 6^\circ$ in $|PA - \theta|$ of the LMC and SMC, respectively, may be within the measurement uncertainties.

5 LARGE-SCALE STRUCTURE OF THE MC SYSTEM

We analyse the large-scale structure of the Clouds by means of the angular distribution of extended objects (adding star clusters and associations in general). Since the Clouds do not have symmetrical structures (Fig. 1), we employ two different approaches in what follows. First, we explore angular slices along nearly perpendicular directions (Section 5.1), and concentric radial distribution (Section 5.2).

5.1 Azimuthal extractions

The position of the extracted slices take advantage of the direction of the prominent LMC bar, and the possible bar/disc structure. The adopted geometry of the extractions is illustrated in Fig. 7. We examine the structure along the LMC bar and in a perpendicular direction, which probes the underlying disc. In the SMC we extract slices along the disc/bar and nearly perpendicular directions. As reference, we take as centres of the slices the geometrical centroids of the LMC bar and the SMC disc/bar (Table 8).

Fig. 8 shows the azimuthal density profiles for the LMC (top left-hand panel) and SMC (bottom left-hand panel). The distance of a given object with the observed equatorial coordinates (α, δ) to the adopted centroid (α_0, δ_0), is computed as $R = \sqrt{[(\alpha - \alpha_0)\cos(\delta)]^2 + (\delta - \delta_0)^2}$. Thus, because of the declination $\delta \approx -70^\circ$ of the Clouds, angular separations in Fig. 8 correspond to $\approx 1/3$ of those implied by the axes of Fig. 1.

As expected, the main LMC structures, such as the bar, the high-surface brightness (HSB) disc and the outer ring, can be detected in the profiles. The SMC profiles appear to be described essentially by exponential discs. While both SMC profiles are almost symmetrical with respect to the adopted centroid, the prominent LMC structures introduce significant asymmetries, both with respect to the bar centroid and between the perpendicular slices. The LMC bar is a factor ≈ 5 denser (in terms of the number of objects per area) than the HSB disc. The central excess in the perpendicular LMC profile corresponds to part of the bar. In the SMC, the average density of the bar/disc profile is a factor ≈ 5 denser than that of the nearly perpendicular direction.

In any case, we build as well pseudo-symmetrical profiles by folding the opposite sides of the azimuthal extractions over the respective centres. In this process, symmetrical points that occur at the same bin of distance to centroid are averaged out. The mirrored radial profiles are shown in the right-hand panels of Fig. 8,

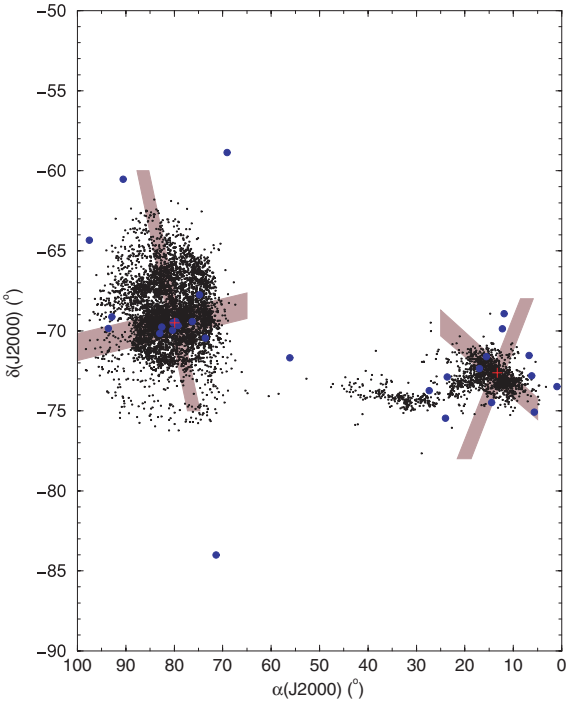

Figure 7. Geometry of the extracted angular slices. The wider stripe in the LMC traces the bar and beyond, while in the SMC it follows the disc/bar direction. Nearly perpendicular slices were also extracted. Slices are centred on the geometrical centroids (plus signs) of the LMC bar and SMC bar/disc structure. Clusters older than 4 Gyr are shown as blue circles.

Table 8. Centroid coordinates of the different reference systems.

Reference System	$\alpha(J2000)$ (h m s)	$\delta(J2000)$ (° ′ ″)	$\Delta\alpha$ (arcmin)	$\Delta\delta$ (arcmin)
LMC combined	05:31:28.8	−69:22:30	–	–
LMC clusters	05:31:00.0	−69:22:48	−7.2	−3.0
SMC combined	00:52:31.2	−73:15:00	–	–
SMC clusters	00:53:28.8	−73:07:48	+15.0	+7.2
LMC bar	05:19:36.6	−69:07:08	−178	−7.7
SMC bar/disc	00:53:10.3	−72:37:12	+9.8	+37.8

Notes. The offsets of the centroid coordinates derived from the cluster distribution with respect to the combined (clusters+associations) distribution are given by $\Delta\alpha$ and $\Delta\delta$. The last two lines correspond to the geometrical centroids of the LMC bar and SMC bar/disc.

where the main structural features can be seen as well. We fit these profiles with an exponential-disc function adapted to number counts, $\sigma(R) = \sigma_{0D}\, e^{-(R/R_D)}$, where σ_{0D} represents the number-density of objects at the centre, and R_D is the disc scale length. As expected, both SMC profiles are well fit by exponential-discs, with the scale lengths $R_D = 0.^\circ 52 \pm 0.^\circ 03 \approx 0.54 \pm 0.03$ kpc and $0.^\circ 44 \pm 0.^\circ 08 \approx 0.46 \pm 0.08$ kpc, respectively for the bar/disc parallel and nearly perpendicular profiles. The LMC profiles, on the other hand, require two exponential-discs each to account for the dense structures. Thus, the profile parallel to the bar can be represented by the disc scale lengths $R_D = 3.^\circ 1 \pm 0.^\circ 3 \approx 2.7 \pm 0.3$ kpc and $0.^\circ 49 \pm 0.^\circ 05 \approx 0.43 \pm 0.04$ kpc, for the bar region and beyond the bar limits, respectively. In the nearly perpendicular direction, two discs are also necessary, but in this case the inner one (within the bar limits) corresponds to the HSB disc. In this case, the

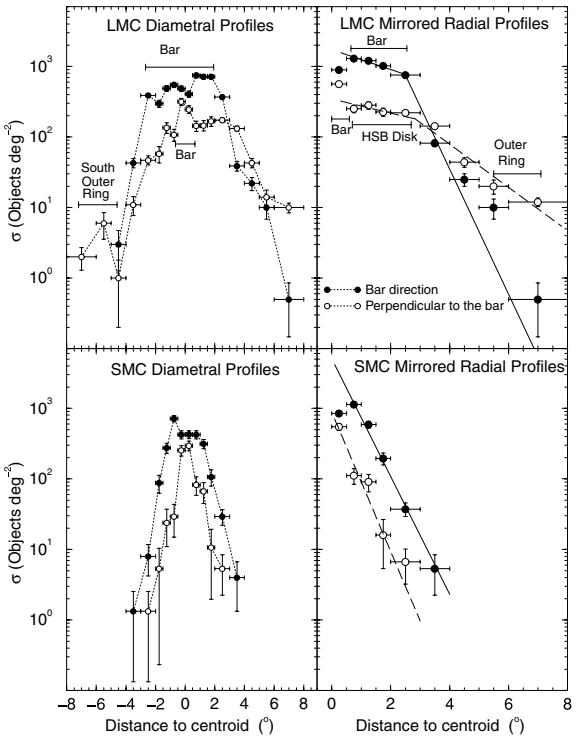

Figure 8. Left-hand panels: azimuthal profiles extracted along the LMC bar and SMC bar/disc directions (filled circles). Profiles extracted in nearly perpendicular directions are also shown (empty circles). Right-hand panels: radial profiles built from the azimuthal ones by folding them over the centroid. Main LMC structures are indicated. Fits with exponential discs are shown.

number-density excesses over the disc profile correspond to the additional outer disc (Fig. 1). We derive $R_D = 4.^\circ4 \pm 1.^\circ2 \approx 3.8 \pm 1.0$ kpc and $1.^\circ42 \pm 0.^\circ15 \approx 1.2 \pm 0.1$ kpc for the inner and outer parts of the perpendicular profile. The innermost points (Fig. 8) in both profiles were excluded from the fits.

There is evidence that the Magellanic Clouds have complex spatial structure. Indeed, the LMC has an inclined disc-like structure (e.g. Olsen & Salyk 2002), which is warped (e.g. Nikolaev et al. 2004), and flared (e.g. Alves & Nelson 2000). Besides, the deprojected LMC structure is elliptical, being more extended along the north–south direction (van der Marel 2001). The SMC appears to have a three-dimensional structure more extended along the line of sight (Crowl et al. 2001). The present analysis (Fig. 8) is based on the angular distribution of the objects in both Clouds. Thus, it is possible that part of the differences detected in the two perpendicular directions in both Clouds arises from their intrinsic properties and projection effects.

5.2 Concentric radial distribution

Alternatively, we analyse the spatial distribution of the extended objects by means of the radial density profiles (RDPs). The RDPs correspond to the projected radial surface-density, that is, the number-density of objects contained in concentric rings around the LMC and SMC centroids. The underlying assumption for this kind of analysis, which is mostly applied to star clusters, is that the structures should present an important degree of radial symmetry. This is not the case of the Clouds, as discussed in previous sections. In any case, RDPs still can be used as probes of the radial distribution of objects averaged over all azimuthal directions and, consequently, of the large-scale structure.

Table 8 gives the LMC and SMC centroid coordinates derived for the spatial distribution of the combined clusters+associations (and related objects), as well as those corresponding to the clusters separately. These centroids correspond to the region where the maximum number-density of objects in each class occurs. In the LMC the cluster centroid is shifted ≈7 and ≈3 arcmin to the west and south, respectively, with respect to the combined distribution centroid. The offset in the SMC is about twice as large, but in the opposite directions. We recall that the position of 30 Dor (R 136) is $\alpha(J2000) = 05^{\rm h}38^{\rm m}42^{\rm s}$, and $\delta(J2000) = -69^\circ06'02''$, thus somewhat to the east and north of the centroids in Table 8 (Fig. 1).

It is worth noting that a centroid definition depends on which tracer is used. For instance, de Vaucouleurs & Freeman (1972) obtained $\alpha(J2000) = 5^{\rm h}23^{\rm m}24^{\rm s}$ and $\delta(J2000) = -69^\circ44'00''$ as the optical centre of the LMC bar. With stellar density contours in the infrared, van der Marel (2001) obtained $\alpha = 5^{\rm h}25^{\rm m}05^{\rm s}$ and $\delta = -69^\circ47'00''$ as the LMC centre. Finally, Kim et al. (1998) found the LMC H I kinematic centre to lie at $\alpha = 5^{\rm h}17^{\rm m}24^{\rm s}$ and $\delta = -69^\circ02'00''$. Thus, our LMC bar centroid (Table 8), which is particularly sensitive to the distribution of young clusters and associations, lies somewhat to the north-west of the optical value provided by de Vaucouleurs & Freeman (1972). The present LMC centroid (Table 8) lies to the east of those of van der Marel (2001) (≈$6^{\rm m}$) and Kim et al. (1998) (≈$14^{\rm m}$), and halfway (≈22 arcmin) between them in declination. As for the SMC, Westerlund (1990) reported $\alpha(J2000) = 0^{\rm h}49^{\rm m}47^{\rm s}$ and $\delta(J2000) = -72^\circ55'40''$ as the optical centre, which lies ≈15 arcmin and ≈$3^{\rm m}$ to the north-west of the centroid derived in this work (Table 8).

We build the RDPs with the centroid coordinates derived for the combined distributions (Table 8). They are shown in Fig. 9, with the combined clusters+associations (top panels) and clusters, separately (bottom panels). Many of the catalogue objects are young, and the corresponding RDPs should represent the relatively recent spatial distribution, $t \lesssim 200$ Myr (Bica et al. 1996).

At first sight, the RDPs (Fig. 9) present similar shapes, with a relatively flat and extended central region followed by a steep decline towards large galactocentric radii. As expected from its larger size, the LMC RDPs reach a distance of $R \approx 8^\circ$ from the centre, while in the SMC, $R \lesssim 3^\circ$.

As a first approach to describe the LMC and SMC structures implied by the RDPs, by means of an analytical function, we test an exponential-disc profile. In all cases, the overall fit fails to reproduce important RDP features. In particular, it overestimates the density of objects especially in the central parts and external region, and underestimates it in the mid region. Fit parameters are given in Table 9. In any case, this kind of fit suggests that the LMC disc-scale length is ≈1°, about twice the SMC value. We also try the $R^{1/4}$ law (de Vaucouleurs 1948), but as shown for the LMC RDP (panel a), it fails completely. Obviously, a combination of both would not either describe the profiles. One conclusion, drawn from such a statistically comprehensive catalogue, is that the (angular-average) large-scale structure of both interacting irregular galaxies does not follow the classical disc and/or spheroidal laws.

Alternatively, we also test a three-parameter profile based on the King (1966) law, which usually describes the structure of star clusters, especially the Galactic GCs and open clusters, by means of the surface-brightness distribution. Formally, we express the adopted King-like profile as $\sigma(R) = \sigma_{0\rm K}[1/\sqrt{1+(R/R_c)^2} - 1/\sqrt{1+(R_t/R_c)^2}]^2$, where R_c and R_t are the core and tidal radii,

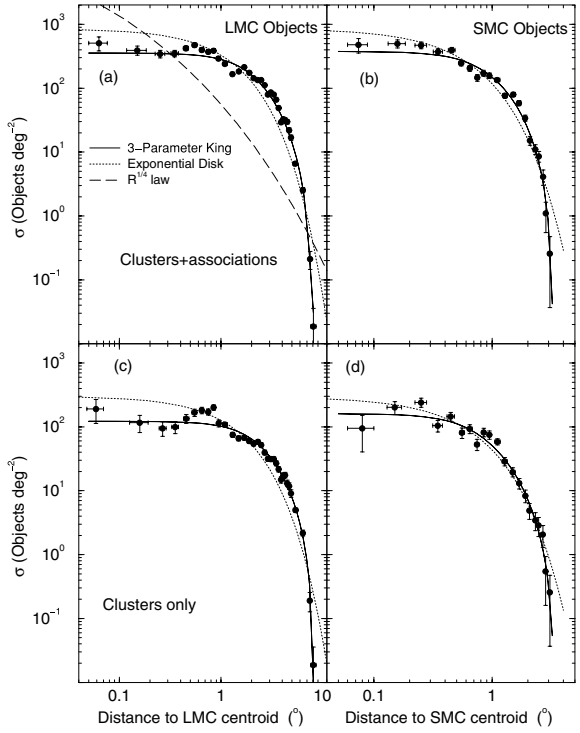

Figure 9. Radial density profiles for the clusters and associations combined (top panels) and clusters separately (bottom panel), located in the LMC (left-hand panel) and SMC (right-hand panel). Fits with the three-parameter King (solid line) and exponential disc (dotted) profiles are shown in all panels. Panel (a) contains a tentative fit with the $R^{1/4}$ law (dashed line).

respectively, and σ_{0K} is the central density of objects. Qualitatively, the corresponding profiles reproduce well the observed RDPs over the full radial range (Fig. 9). Within uncertainties, the structural parameters implied by the combined clusters+associations and clusters alone RDPs are similar (Table 9). For the LMC we derive a core radius $R_c \approx 2.^\circ6$ which, at the LMC distance (≈50 kpc), corresponds to $R_c \approx 2.3$ kpc; for the tidal radius we derive $R_t \approx 8.^\circ1 \approx 7$ kpc. Similar considerations for the SMC (≈60 kpc) lead to $R_c \approx 1^\circ \approx 1$ kpc, and $R_t \approx 3.^\circ3 \approx 3.5$ kpc. Thus, in absolute units, the SMC structural radii correspond to about half of the LMC ones. Finally, the concentration parameters $c_p = \log(R_t/R_c)$, in all cases, are comparable to those of the least concentrated Galactic GCs (see, e.g. fig. 7 in Bonatto et al. 2007).

King profiles usually describe the structure of virialized systems, such as the old Galactic GCs, but many of the LMC and SMC objects used in the above analysis are young. However, we note that the structure of some young Galactic star clusters have been shown to follow the King profile as well, e.g. the ∼1.3 Myr open cluster NGC 6611 (Bonatto, Santos & Bica 2006) and NGC 4755 (Bonatto et al. 2006b), with ∼10 Myr of age. Ironically, the best fit to the average radial distribution of objects in both Clouds is given by the King-like profile, which is not usually applied to the structure of galaxies.

Each Cloud harbours about half of the 29 old star clusters present in the catalogue (electronic Table 3; Fig. 1). Such clusters are much older than the time elapsed since the last encounter between both Clouds (e.g. Bekki & Chiba 2007), and they can be used to probe whether the present-day spatial distribution of the old clusters retains information on the early-Cloud structure. Two of these are the very distant GCs NGC 1841 and Reticulum, at $R \approx 10^\circ$ (Fig. 1), which are likely LMC members (Suntzeff et al. 1992). We consider for this analysis a composite RDP, in which we compute for each old star cluster the distance to the nearest MC centroid. The combined LMC and SMC RDP is shown in Fig. 10. At first sight, it appears to represent a more extended structure than those discussed in Fig. 9, but the extension may be caused by the two distant GCs. In any case, the exponential disc, with a scale-length of about 2°, now appears to describe the full radial range of the RDP somewhat better than the three-parameter King profile, while the $R^{1/4}$ law fails altogether. The more extended character of this RDP is reflected on the fit structural parameters, which are larger than those derived with the younger objects (Table 9).

6 SUMMARY AND CONCLUSIONS

The primary goal of this paper is to update the catalogue of extended objects in the Magellanic System. With the recent addition of HST, CCD mosaics and survey data, the number of known objects in the Clouds now reaches 9503, which represents a relatively substantial increase of ≈12 per cent with respect to the previous versions (Bica & Schmitt 1995; Bica et al. 1999; Bica & Dutra 2000). It now includes H I shells and supershells, cross-identifications with the previous literature, and subsequently discovered objects.

Such a number of objects is large enough to allow for a statistically significant analysis of environmental effects on the distribution of structural parameters among the different classes of objects, in the LMC, SMC and Bridge tidal fields separately. Star clusters present similar distributions of structural parameters in the three MC subsystems. SMC associations (and related objects, emission nebulae, and H I shells and supershells), on the other hand, tend to be larger and more circular than in the LMC. We also detect evidence that the apparent diameter of clusters and associations increase with the distance to each Cloud centroid. The ellipticity presents the opposite trend, especially in the SMC. These relations are consistent with the

Table 9. Structural parameters measured in the RDPs with the three-parameter King and exponential-disc profiles (Fig. 9).

	$\sigma_{0K}[1/\sqrt{1+(R/R_c)^2} - 1/\sqrt{1+(R_t/R_c)^2}]^2$					$\sigma_{0D} \times e^{-(R/R_D)}$		
RDP	σ_{0K} (Obj. deg^{-2})	R_c (deg)	R_t (deg)	c_p	CC	σ_{0D} (Obj. deg^{-2})	R_D (deg)	CC
(1)	(2)	(3)	(4)	(5)	(6)	(7)	(8)	(9)
LMC combined	705 ± 30	2.4 ± 0.2	7.9 ± 0.2	0.52	0.982	860 ± 108	1.0 ± 0.05	0.898
LMC clusters	261 ± 11	2.8 ± 0.2	8.4 ± 0.2	0.48	0.984	303 ± 39	1.1 ± 0.05	0.897
SMC combined	820 ± 62	1.1 ± 0.1	3.3 ± 0.1	0.48	0.978	861 ± 115	0.5 ± 0.03	0.978
SMC clusters	293 ± 27	0.9 ± 0.1	3.4 ± 0.2	0.58	0.967	295 ± 37	0.5 ± 0.03	0.947
Old clusters	1.4 ± 0.3	4.0 ± 1.5	11.0 ± 0.5	0.44	0.912	1.2 ± 0.3	1.9 ± 0.2	0.943

Notes. Col. 5: concentration parameter, $c_p = \log(R_t/R_c)$. Col. 6: fit correlation coefficient. Combined: star clusters+associations.

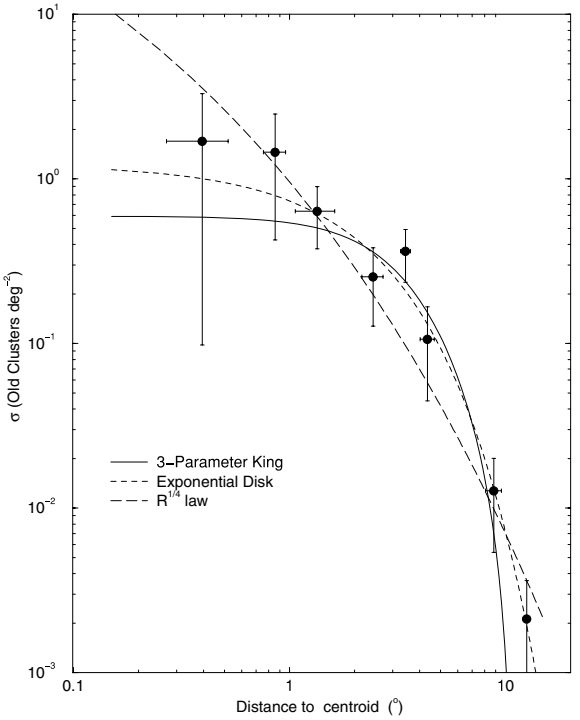

Figure 10. Same as Fig. 9 for the old star clusters of the LMC and SMC. The LMC and SMC individual RDPs have been merged to increase the statistics. The exponential disc appears to be the best fit to the RDP.

relative strengths of the LMC, SMC and Bridge tidal fields. Indeed, the standard model of Bekki & Chiba (2007) assumes the masses $M_{\rm LMC} = 2 \times 10^{10}\,{\rm M}_{\odot}$ and $M_{\rm SMC} = 3 \times 10^{9}\,{\rm M}_{\odot}$ for the LMC and SMC, respectively. Obviously, the Bridge is less massive than the SMC. Such masses can produce significant tidal stress on star clusters and associations, depending on their location.

With respect to the angular distribution of objects, number-density profiles extracted along the LMC bar and in a perpendicular direction can be reasonably well represented by two exponential discs, one for the bar region and the other for the outer parts of the profile (Fig. 8). Disc scale-lengths parallel to the bar are ≈2.7 kpc and ≈0.4 kpc, for the bar region and beyond, respectively. In the perpendicular direction they are ≈3.8 and ≈1.2 kpc, for the high-surface brightness disc and outer ring, respectively. Similar profiles extracted along equivalent directions in the SMC follow a single exponential disc with ≈0.5 kpc of scale-length.

Alternatively, when (angular-averaged) radial number-density profiles are considered, the large-scale structure of both Clouds appears to be best described by a three-parameter King-like function, characterized by core and halo substructures. In this case, the LMC core and tidal radii are $R_{\rm c} \approx 2\overset{\circ}{.}6$ and $R_{\rm t} \approx 8\overset{\circ}{.}2$, respectively; SMC values are a factor ≈0.4 of the LMC ones. In absolute scale, LMC values are $R_{\rm c} \approx 2.3$ kpc and $R_{\rm t} \approx 7.2$ kpc, while SMC ones are about half of these. The tidal/core radii ratio in both Clouds imply low concentration parameters, comparable to those of sparse Galactic GCs.

What emerges from the present work is a scenario where the present-day, (angular-averaged) large-scale structures of both Clouds appear to behave as tidally truncated systems (which is not unexpected, since they are Milky Way satellites), characterized by well-defined core and halo substructures. This picture comes about despite the fact that both Clouds are not spherical systems (Fig. 1). Thus, they have undergone severe tidal perturbation when the last dynamical and hydrodynamical interaction between the Clouds took place, about 200 Myr ago (Bekki & Chiba 2007). Taken isolately, the older LMC and SMC star clusters, on the other hand, appear to be distributed as an exponential disc. This distribution is possibly reminiscent of the Clouds structure prior to the last interaction.

The LMC/SMC interaction is not unusual in the local Universe. They can be classified into the minor-merger interaction picture, which involves high and low-mass galaxies (e.g. Ferreiro & Pastoriza 2004, and references therein). A series of examples of such interactions involving galaxies with prominent bulge and disc has been studied in that paper. Some of the disc galaxies developed the double-disc structure, similarly to the present case of the LMC.

ACKNOWLEDGMENTS

We acknowledge partial support from CNPq (Brazil). We thank the anonymous referee for interesting suggestions.

REFERENCES

Alcaino G., Alvarado F., Kurtev R., 2003, A&A, 407, 919
Alves D. R., Nelson C. A., 2000, ApJ, 542, 789
Battinelli P., Demers S., 1992, AJ, 104, 1458
Bekki K., Chiba M., 2007, PASA, 24, 21
Bellazzini M., Pancino E., Ferraro F. R., 2005, A&A, 435, 871
Bhatia R. K., Hatzidimitriou D., 1988, MNRAS, 230, 215
Bica E., Dutra C. M., 2000, AJ, 119, 1214
Bica E., Schmitt H., 1995, ApJS, 101, 41
Bica E., Clariá J. J., Dottori H., Santos J. F. C., Jr., Piatti A. E., 1996, ApJS, 102, 57
Bica E., Schmitt H., Dutra C. M., Oliveira H. L., 1999, AJ, 117, 238
Bica E., Bonatto C., Barbuy B., Ortolani S., 2006, A&A, 450, 105
Blair W. P., Ghavamian P., Sankrit R., Danforth C. W., 2006, ApJS, 165, 480
Bojicic I. S., Filipovic M. D., Parker Q. A., Payne J. L., Jones P. A., Reid W., Kawamura A., Fukui Y., 2007, MNRAS, 378, 1237
Bonatto C., Bica E., 2005, A&A, 437, 483
Bonatto C., Bica E., 2007, A&A, 473, 445
Bonatto C., Bica E., 2008, A&A, 479, 741
Bonatto C., Santos J. F. C., Jr., Bica E., 2006, A&A, 445, 567
Bonatto C., Kerber L. O., Bica E., Santiago B. X., 2006a, A&A, 446, 121
Bonatto C., Bica E., Ortolani S., Barbuy B., 2006b, A&A, 453, 121
Bonatto C., Bica E., Ortolani S., Barbuy B., 2007, MNRAS, 381, L45
Bowyer S., Sasseen T. P., Wu X., Lampton M., 1995, ApJS, 96, 461
Chu Y.-H., Kennicutt R. C., Snowden S. L., Smith R. C., Williams R. M., Bomans D. J., 1997, PASP, 109, 554
Crowl H. H., Sarajedini A., Piatti A. E., Geisler D., Bica E., Clariá J. J., Santos J. F. C., Jr., 2001, AJ, 122, 220
Da Costa G. S., 1991, IAUS, 148, 183
Da Costa G. S., 1999, IAUS, 190, 446
Davies R. D., Elliott K. H., Meaburn J., 1976, MmRAS, 81, 89
de Vaucouleurs G., 1948, Ann. Astrophys., 11, 247
de Vaucouleurs G., Freeman K. C., 1972, VA, 14, 163
Dickel J. R., Williams R. M., Carter L. M., Milne D. K., Petre R., Amy S. W., 2001, AJ, 122, 849
Dieball A., Müller H., Grebel E. K., 2002, A&A, 391, 547
Dottori H., Bica E., Clariá J. J., Puerari I., 1996, ApJ, 461, 742
Dutra C. M., Bica E., Clariá J. J., Piatti A. E., 1999, MNRAS, 305, 373
Ferreiro D. L., Pastoriza M. G., 2004, A&A, 428, 837
Gieles M., Portegies Zwart S. F., Baumgardt H., Athanassoula E., Lamers H. J. G. L. M., Sipior M., Leenaarts J., 2006, MNRAS, 371, 793
Gouliermis D., Kontizas M., Kontizas E., Korakitis R., 2003, A&A, 405, 111
Gouliermis D., Quanz S. P., Henning T., 2007, ApJ, 665, 306

Harris W. E., 1996, AJ, 112, 1487
Hatzidimitriou D., Stanimirovic S., Maragoudaki F., Staveley-Smith L., Dapergolas A., Bratsolis E., 2005, MNRAS, 360, 1171
Henize K. G., 1956, ApJS, 2, 315
Henize K. G., Westerlund B. E., 1963, ApJ, 137, 747
Hennekemper E., Gouliermis D. A., Henning T., Brandner W., Dolphin A. E., 2008, ApJ, 672, 914
Heydari-Malayeri M., Charmandaris V., Deharveng L., Rosa M. R., Zinnecker H., 1999, A&A, 347, 841
Heydari-Malayeri M., Royer P., Rauw G., Walborn N. R., 2000, A&A, 361, 877
Heydari-Malayeri M., Charmandaris V., Deharveng L., Rosa M. R., Schaerer D., Zinnecker H., 2001, A&A, 372, 527
Heydari-Malayeri M., Charmandaris V., Deharveng L., Meynadier F., Rosa M. R., Schaerer D., Zinnecker H., 2002, A&A, 381, 941
Heydari-Malayeri M., Meynadier F., Walborn N. R., 2003, A&A, 400, 923
van der Heyden K. J., Bleeker J. A. M., Kaastra J. S., 2004, A&A, 421, 1031
Hodge P., 1985, PASP, 97, 530
Hodge P., 1986, PASP, 98, 1113
Hodge P. W., Sexton J. A., 1966, AJ, 71, 363
Kim S., Staveley-Smith L., Dopita M. A., Freeman K. C., Sault R. J., Kesteven M. J., McConnell D., 1998, ApJ, 503, 674
Kim S., Dopita M. A., Staveley-Smith L., Bessell M. S., 1999, AJ, 118, 2797
King I., 1966, AJ, 71, 64
Kontizas M., Morgan D. H., Hatzidimitriou D., Kontizas E., 1990, A&AS, 84, 527
Kron G. E., 1956, PASP, 68, 125
Lazendic J. S., Dickel J. R., Jones P. A., 2003, ApJ, 596, 287
Lindsay E. M., 1958, MNRAS, 118, 172
Lindsay E. M., 1961, AJ, 66, 169
Lucke P. B., Hodge P. W., 1970, AJ, 75, 171
Lyngå G., 1982, A&A, 109, 213
Lyngå G., Westerlund B. E., 1963, MNRAS, 127, 31
Mackey A. D., Gilmore G. F., 2003, MNRAS, 338, 85
Mackey A. D., Gilmore G. F., 2004, MNRAS, 352, 153
Mackey A. D., Payne M. J., Gilmore G. F., 2006, MNRAS, 369, 921
Meynadier F., Heydari-Malayeri M., Walborn N. R., 2005, A&A, 436, 117
Mighell K. J., Sarajedini A., French R. S., 1998, AJ, 116, 2395
Muller E., Parker Q. A., 2007, PASA, 24, 69
Muller E., Staveley-Smith L., Zealey W., Stanimirovic S., 2003, MNRAS, 339, 105
Nakajima Y. et al., 2005, AJ, 129, 776
Nikolaev S., Drake A. J., Keller S. C., Cook K. H., Dalal N., Griest K., Welch D. L., Kanbur S. M., 2004, ApJ, 601, 260
Nota A. et al., 2006, ApJ, 640, 29
Oey M. S., Parker J. S., Mikles V. J., Zhang X., 2003, AJ, 126, 2317
de Oliveira M. R., Dutra C. M., Bica E., Dottori H., 2000, A&AS, 146, 57
Olsen K. A. G., Salyk C., 2002, AJ, 124, 2045
Olszewski E. W., Aaronson M., Schommer R. A., 1987, AJ, 93, 565
Piatti A. E., Santos J. F. C., Jr., Clariá J. J., Bica E., Sarajedini A., Geisler D., 2001, MNRAS, 325, 792
Piatti A. E., Sarajedini A., Geisler D., Bica E., Clariá J. J., 2002, MNRAS, 329, 556
Piatti A. E., Sarajedini A., Geisler D., Seguel J., Clark D., 2005, MNRAS, 358, 1215
Piatti A. E., Sarajedini A., Geisler D., Gallart C., Wischnjewsky M., 2007, MNRAS, 381, L84
Pietrzynski G., Udalski A., 1999, AcA, 49, 433
Pietrzynski G., Udalski A., 2000, AcA, 50, 355
Pietrzynski G., Udalski A., Kubiak M., Szymanski M., Wozniak P., Zebrun K., 1998, AcA, 48, 175
Pietrzynski G., Udalski A., Kubiak M., Szymanski M., Wozniak P., Zebrun K., 1999, AcA, 49, 521
Reid W. A., Payne J. L., Filipovic M. D., Danforth C. W., Jones P. A., White G. L., Staveley-Smith L., 2007, MNRAS, 367, 1379
Sabbi E. et al., 2007, AJ, 133, 44
Santiago B. X., Elson R. A. W., Sigurdsson S., Gilmore G. F., 1998, MNRAS, 295, 860
Schaefer B. E., 2008, AJ, 135, 112
Schmalzl M., Gouliermis D., Dolphin A. E., Henning T., 2008, ApJ, 681, 290
Shapley H., Lindsay E. M., 1963, IrAJ, 6, 74
Staveley-Smith L., Sault R. J., Hatzidimitriou D., Kesteven M. J., McConnell D., 1997, MNRAS, 289, 225
Suntzeff N. B., Schommer R. A., Olszewski E. W., Walker A. R., 1992, AJ, 104, 1743
Tadross A. L., Werner P., Osman A., Marie M., 2002, NewAst, 7, 553
Testor G., Llebaria A., Debray B., 1988, Msgr, 54, 43
Testor G., Lemaire J. L., Field D., Diana S., 2006, A&A, 453, 517
Testor G., Lemaire J. L., Kristensen L. E., Field D., Diana S., 2007, A&A, 469, 459
Udalski A., 2003, Acta Astron., 53, 291
van den Bergh S., Morbey C., Pazder J., 1991, ApJ, 375, 594
van der Marel R. P., 2001, AJ, 122, 1827
Walborn N. R., Blades C. J., 1997, ApJSS, 112, 457
Walborn N. R., Barbá R. H., Brandner W., Rubio M., Grebel E. K., Probst R. G., 1999a, AJ, 117, 225
Walborn N. R., Drissen L., Parker J. W., Saha A., MacKenty J. W., White R. L., 1999b, AJ, 118, 1684
Walborn N. R., Maìz-Apellániz J., Barbá R. H., 2002, AJ, 124, 1601
Westerlund B. E., 1990, A&ARv, 2, 29
Westerlund B. E., Henize K. G., 1963, PASP, 75, 332
Williams R. M., Chu Y.-H., Gruendl R., 2006, AJ, 132, 1877

SUPPORTING INFORMATION

Additional Supporting Information may be found in the online version of this article.

Table 3. Star clusters.
Table 4. Associations.
Table 5. Emission nebulae.
Table 6. H I shells and supershells.

Pase note: Blackwell Publishing are not responsible for the content or functionality of any supporting information supplied by the authors. Any queries (other than missing material) should be directed to the corresponding author for the article.

This paper has been typeset from a TEX/LATEX file prepared by the author.